Journal of Power Sources 194 (2009) 961–966

Contents lists available at ScienceDirect

Journal of Power Sources

journal homepage: www.elsevier.com/locate/jpowsour

Intermediate temperature single-chamber methane fed SOFC based on Gd doped ceria electrolyte and $La_{0.5}Sr_{0.5}CoO_{3-\delta}$ as cathode

M. Morales[a,b], S. Piñol[a,*], M. Segarra[b]

[a] Institut de Ciència de Materials de Barcelona (CSIC), Campus de la UAB, Bellaterra, E-08193, Barcelona, Spain
[b] Departament de Ciència de Materials i Enginyeria Metallúrgica, Facultat de Química, Universitat de Barcelona, Diagonal 647, E-08028, Barcelona, Spain

ARTICLE INFO

Article history:
Received 5 December 2008
Received in revised form 28 April 2009
Accepted 15 May 2009
Available online 22 May 2009

Keywords:
SOFC
Single chamber fuel cells
Electrolyte-supported
Ceria
Cobaltite
Methane

ABSTRACT

Single-chamber fuel cells with electrodes supported on an electrolyte of gadolinium doped ceria $Ce_{1-x}Gd_xO_{2-y}$ with $x = 0.2$ (CGO) 200 μm thickness has been successfully prepared and characterized. The cells were fed directly with a mixture of methane and air. Doped ceria electrolyte supports were prepared from powders obtained by the acetyl-acetonate sol–gel related method. Inks prepared from mixtures of precursor powders of NiO and CGO with different particle sizes and compositions were prepared, analysed and used to obtain optimal porous anodes thick films. Cathodes based on $La_{0.5}Sr_{0.5}CoO_3$ perovskites (LSCO) were also prepared and deposited on the other side of the electrolyte by inks prepared with a mixture of powders of LSCO, CGO and AgO obtained also by sol–gel related techniques. Both electrodes were deposited by dip coating at different thicknesses (20–30 μm) using a commercial resin where the electrode powders were dispersed. Finally, electrical properties were determined in a single-chamber reactor where methane, as fuel, was mixed with synthetic air below the direct combustion limit. Stable density currents were obtained in these experimental conditions. Temperature, composition and flux rate values of the carrier gas were determinants for the optimization of the electrical properties of the fuel cells.

1. Introduction

A new type of SOFC, the single-chamber fuel cell, which shows very high current density at relatively low temperatures (450–630 °C), has been developed by different research groups [1–10]. The main difference between the one-chamber fuel cells and the conventional two-chamber fuel cells is that, in the former, both electrodes are simultaneously in contact with both the fuel and the air. The advantages of such SOFCs are that they do not need expensive materials, they are very simple to fabricate, and it is very easy to assemble them into multiple stacks. These SOFCs can work directly with hydrocarbons (internal reforming) because the temperature at which they operate is adequate for hydrocarbon reforming in the anode. Moreover, the poisoning of the Ni by carbon or sulphur is not possible due to the presence of oxygen on the anode electrode which avoids the poisoning of the catalyst.

Solid oxide electrolytes based on ceria doped materials are considered to be one of the most promising candidate materials for use in single-chamber intermediate temperature solid oxide fuel cells, because they offer considerably higher ionic conductivity than YSZ in the range of 450–800 °C. The substitution of Ce^{4+} by suitable trivalent cations such as Gd^{3+}, Sm^{3+}, Y^{3+} or La^{3+} has been done in ceria-based electrolytes because enhances the chemical stability, increases the ionic conductivity and suppresses the reducibility of ceria-based materials. The most effective substitutes are Gd_2O_3 and Sm_2O_3 possibly due to the fact that they minimize the changes in lattice parameter.

Both, electrolyte-supported and anode-supported fuel cells have been reported for these doped ceria fuel cells based in one chamber reactor. However, there is some difficulty to find stable cathodes in one-chamber fuel cells under the proposed reducing conditions. Hibino et al. [8] reported a relatively high peak power density at 500 °C for an electrolyte-supported fuel cell using $Sm_{0.5}Sr_{0.5}CoO_{3-\delta}$ mixed with $Ce_{0.8}Sm_{0.2}O_{1.9}$ (SSC + CSO) as the cathode and ethane as the fuel. However, they found that this cathode was incompatible with propane at temperatures higher than 450 °C. It should be noted that, because of the heat release during partial exothermic oxidation at the anode, the actual temperature of the fuel cell is higher than the furnace temperature, depending on the operation conditions [9]. This self-heating in single-chamber fuel cells explains the higher power densities obtained from single-chamber, as compared with dual-chamber, fuel cells at lower apparent furnace temperatures. Shao et al. have presented a new cathode ($Ba_{0.5}Sr_{0.5}Co_{0.8}Fe_{0.2}O_{3-\delta}$), which works well with propane or methane as fuel in an anode-supported single chamber fuel cell based on CSO electrolytes generating power

* Corresponding author. Tel.: +34 93 580 18 53; fax: +34 93 580 57 29.
E-mail address: salva@icmab.es (S. Piñol).

0378-7753/$ – see front matter © 2009 Elsevier B.V. All rights reserved.
doi:10.1016/j.jpowsour.2009.05.027

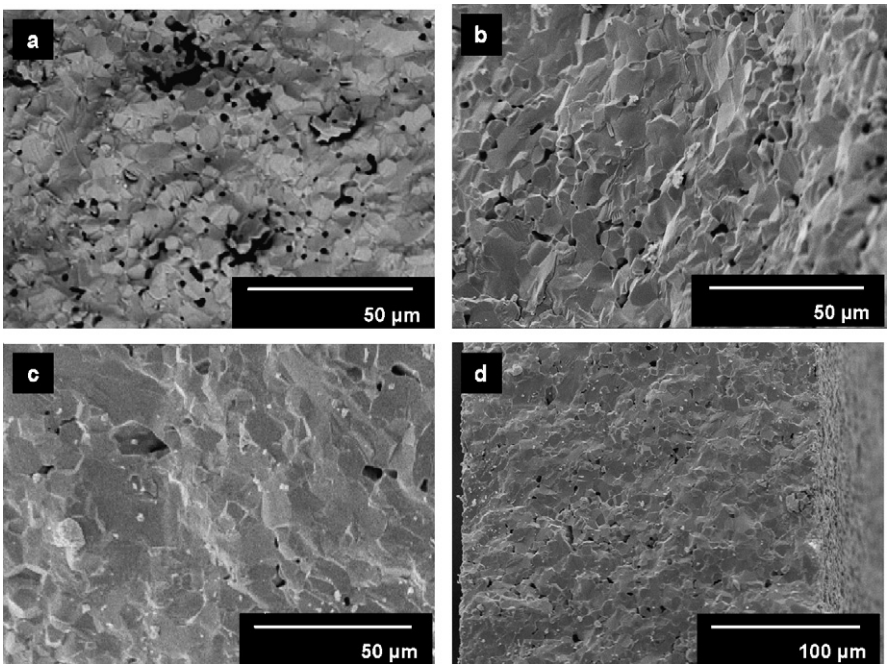

Fig. 1. Variation of the porosity as a function of CGO/Co composition for different electrolytes calcined at a constant temperature of 1400 °C. (a) 100% CGO, (b) 99% CGO + 1% Co, (c and d) 98% CGO + 2% Co at different magnifications.

densities above 700 mW cm^{-2} at 760–790 °C using methane as fuel and He as carrier gas [10–12]. We show in the present work that the cathode $La_{0.5}Sr_{0.5}CoO_3$ (LSCO) is also stable up to 800 °C in an electrolyte-supported single chamber fuel cell with methane as fuel diluted in air. We have obtained power densities up to 300 mW cm^{-2} at 780 °C in methane/air mixtures. This lower density power may be attributed to the thickness of the electrolyte. Moreover, we have found that fuel cells with LSCO as cathode are also stable with anode-supported CGO electrolyte with propane as fuel mixed in air and operating at lower temperatures (~640 °C) [13].

Some authors have reported that ceria-gadolinia (CGO) possesses the highest values of ionic conductivity with respect to other ceria-doped electrolytes [14] and this was confirmed by computer atomistic simulations based on a combination of coulomb interactions and lattice relaxation [15]. This interaction is dependent on the size of the trivalent additive and the simulations suggest that the optimum radius for the trivalent cation in ceria-based oxide nearly corresponds to Gd^{3+}. Nevertheless, other authors have reported higher values of ionic conductivity for ceria-samaria (CSO) materials [16,17]. It is thus far from clear whether the properties of CGO exceed those of CSO. The differences between results reported by different authors can also be related to differences in powder preparation and the corresponding effects on the relative role of the resistive grain boundary [18,19]. For this reason one may expect some improvements by optimizing the sample preparation method. In this work, we present the results with CGO as electrolyte. The objective of this work is the preparation of a single-chamber fuel cell fed with methane and air with high current densities. We have optimized the electrodes and electrolyte compositions and preparation to obtain high current densities at relatively lower temperatures. For this purpose we have utilized Co additions in the GDC powder preparation in order to increase the density of the electrolyte at lower sintering temperatures without density current losses, as has been demonstrated in our previous work [13,20]. Moreover, we have added AgO in the LSC powder for the cathode preparation to increase the electrical and ionic conductivity of the electrode. We have found that AgO is a good electrical and ionic conductor in the cathode which stabilises the adherence of the cathode to the electrolyte and do not disturbs the fuel-cell working. Probably, AgO catalyses the dissociation of the oxygen molecule but do not catalyses the methane oxidation, because losses in the current density of the fuel cell has not been observed.

2. Experimental

2.1. Powder preparation

Electrolyte and electrode powders for single-chamber fuel cells were prepared by sol–gel related methods. Powders of LSCO for cathodes were prepared by the citrate sol–gel method starting from nitrate solutions of the different elements. The powders for the $Ce_{0.8}Gd_{0.2}O_{1.9}$ electrolytes were prepared by the sol–gel acetyl-acetonate method starting from acetates: $Ce(C_2H_3O_2)_3{\cdot}1.5H_2O$ (Alfa Aesar, 99.9% purity), $Gd(C_2H_3O_2)_3{\cdot}xH_2O$ and $Co(C_2H_3O_2)_2$ (Alfa Aesar, 99.9% purity) as described elsewhere [19]. Finally, powder mixtures of 90% of Ni and 10% of CGO for anodes were prepared from commercial Ni powders (ALDRICH, particle size 2.2–3 μm) and CGO prepared by the acetyl-acetonate method. All of these powders were characterized by XRD before his utilization and the patterns showed no evidences of secondary phases.

2.2. Electrolyte preparation

Cylindrical pellets of CGO electrolytes with different amounts of cobalt additions in order to reduce the sintering temperature (from 0.5% to 4% in weight) 10 mm of diameter and a thickness of ~0.2 mm, were prepared by uniaxial pressing at 3 ton cm^{-2} during 30 s. Then, the pellets were heated between 1350 and 1440 °C during 10 h in order to ensure the electrolyte densification. The microstructural analysis of the sintered samples was performed by scanning electron microscopy (SEM). A homogeneous particle size distribution and a very high density for the CGO electrolyte pellets were found for the CGO electrolytes with ~2% of Co additions. Higher Co addi-

tions do not increase the density of the electrolytes because Co evaporations and/or liquid losses by the crucibles take place [20]. Fig. 1 shows the variation of the porosity as a function of CGO/Co composition for different electrolytes calcined at a constant temperature of 1400 °C during 10 h. We can see that porosity of CGO materials decreases with Co proportion. So, the greatest density of CGO pellets was observed for samples with 2% of Co after 10 h at 1400 °C. Optimal fuel cell electrical properties were also found for this composition after this annealing treatment. We have also studied the variation of the CGO/Co electrolyte grain size as a function of annealing temperature. We have observed that the diameter of the CGO/Co grains increases drastically from 1350 to 1440 °C, but the densification of the electrolyte is not obtained at temperatures below 1340 °C even at higher Co additions. For these reasons, we have prepared the electrolytes characterized in the present work at 1400 °C.

2.3. Electrode preparation

Anodes powders were prepared in an agate mortar from a mixture of Ni + CGO 10% by weight mixed with a commercial resin. We have mixed metallic Ni 99.9% purity, 2.2–3 μm average particle size (ALDRICH) and CGO powders prepared as described above by the sol–gel acetyl-acetonate method. The ink so fabricated was deposited by dip coating on one side of the CGO cylindrical electrolyte and the pellets (anode + electrolyte) were annealed 5 h at 900 °C in Ar/H_2 5% before the cathode deposition on the other electrolyte side in order to obtain good electrical contacts avoiding the Ni oxidation.

For cathode preparation, mixtures of LSCO + CGO 10% by weight were prepared also in an agate mortar from the powders obtained by the sol–gel methods described above. Then, the powders were homogenized with 10% weight of nanometric AgO particles obtained by precipitation in water and mixed with the same commercial resin used for anode preparation. The ink so formed was deposited by dip-coating directly on the other side of the dense CGO electrolyte. Finally, the samples (cylindrical anode/electrolyte/cathode) were annealed at 900 °C for 10 h in argon atmosphere to ensure good electrolyte-electrodes contacts.

2.4. Fuel cell electrical properties

Platinum wires were attached to the electrode surfaces of the fuel cells for current collection using the different ink compositions for anodes and cathodes described above. So, Ni + CGO 10% by weight for anodes and LSCO + CGO 10% + AgO 10% by weight for cathodes were used, respectively. Both anode and cathode contacts were performed with the same ink that was used for electrodes film deposition by dip coating. An additional thermocouple Pt versus Pt–10% Rd was placed in direct contact with the centre of the anode surface in order to determine the real temperature of the fuel cells. The fuel cells were placed in a quartz tube reactor of 23 mm of internal diameter, where a mixture of $N_2 + O_2$ close to the air composition (80:20%, respectively) was circulated at different flux rates from 200 to 450 ml min^{-1}. The influence of methane flux rate for electrochemical evaluation was analysed from 0 to 100 ml min^{-1}. Finally, the fuel cells were heated inside the quartz tube by a tubular furnace. It was found that the fuel cells were operatives at actual temperatures between 675 and 775 °C giving considerable density currents.

The organic part of the inks for electrical contacts was eliminated by the carrier gas during the heating at relatively low temperature (300–500 °C). Electromotive forces (emfs) were measured using a Keithley 617 electrometer with an input resistance of 1014 Ω. The value of current was measured by reading the voltage drop in an auxiliary known resistance. *I–V* characteristics were determined by using the equipment for measuring current and voltage under variable loads.

2.5. Catalytic measurements

For catalytic experiments, 20 mg of the LSCO + CGO 10% + 10% AgO and 20–300 mg of Ni + CGO powders were placed on a gold crucible positioned inside the same horizontal tubular quartz tube of 23 mm internal diameter used for fuel cell characterization and heated at 500 °C h^{-1} from room temperature to 800 °C into the same tubular furnace 30 cm length in methane–air mixtures. Experiments were performed at different atmosphere compositions of N_2, O_2 and CH_4 monitored by mass flow controllers. The stirring rate influence was explored until a total flux rate of gas mixtures ~500 ml min^{-1}. Catalytic activity in front of methane oxidation was analysed by gas chromatography. A part of the gas exiting the reactor was analysed using a gas chromatograph equipped with thermal conductivity detectors. The temperature of the furnace was controlled by a temperature controller, and the temperature of the samples was measured using a Pt versus Pt–10% Rd thermocouple placed in the same experimental conditions that the sample. The catalytic activity of the Pt wires and gold crucibles were negligible due to the very small specific surface area.

3. Results and discussion

3.1. Fuel cells temperature characterization

We have found that the temperature of the fuel cells was approximately the same as that of the furnace at relatively low values, during heating. But, the temperature of the fuel cells is higher once considerable oxidation of methane takes place ($T > 690$ °C). Then, an electromotive force and an electrical current at 0 V appear and the temperature of the fuel cells increases drastically. The actual temperature of the fuel cells was ~35–40 °C higher than the furnace temperature during optimal operation of the fuel cells in our experimental conditions. Similar differences between the temperature of the fuel cells and the temperature of the furnace have been characterized and reported recently in the literature by other authors [9,13]. We have observed that the open circuit voltage (O.C.V.) and the current density drop to zero when the fuel cells operational temperature reaches ~850 °C, which corresponds to a furnace temperature of ~800 °C. This deterioration of the electrical properties could be recovered again by decreasing the temperature of the furnace until 740 °C which corresponds to a fuel cell temperature of 775 °C. We have analysed the atmosphere composition by gas chromatography in these conditions at furnace temperature higher than 800 °C. But, we have found that the O_2 composition inside the quartz tube decreases drastically to zero at these critical temperatures. On the other hand, we have observed the same behaviour when we have analysed the gases inside the quartz tube without the fuel cell device in the same experimental conditions. Then, H_2, CO and CO_2 composition in the atmosphere increases drastically but the O_2 composition decreases to zero and the fuel cells are deactivated due to the low oxygen partial pressure. So, we conclude that homogeneous oxidation of methane takes place in the atmosphere at these higher temperatures and the oxygen supply to the cathode is not possible.

The fuel cells density current seems to be stable at fuel cell temperatures lower than 775 °C and shows the same electrical characteristics after more than 3 h of reaction. Then, the total resistance drops to a few kΩ at 650–775 °C depending on the electrolyte thickness and the active surface of the cathode. Typical values of ~1–3 kΩ were found for a 200 μm thickness electrolyte and an active surface of 10 mm^2.

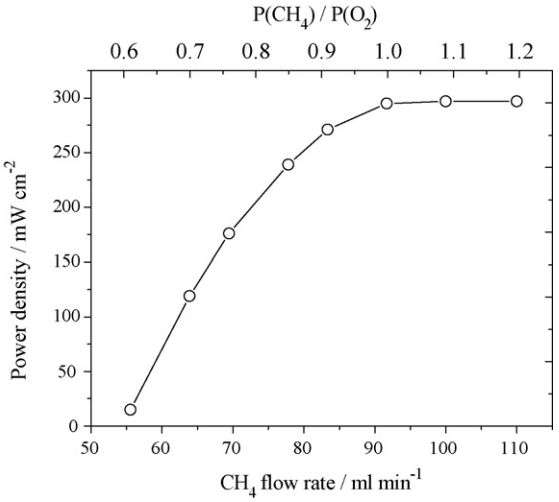

Fig. 2. Power density at 0.4 V and 770 °C cell temperature as a function of fuel to oxygen ratio for a fixed oxygen flow rate of 92 ml min^{-1} and a nitrogen flow rate of 350 ml min^{-1}.

3.2. Electrical measurements

In a first series of experiments, we have explored the influence of the CH_4/O_2 ratio on the electrical properties of the fuel cells at a constant voltage load of 0.4 V and a furnace temperature of 740 °C. So, we have increased the CH_4 flow rate from 0 to 110 ml min^{-1} maintaining a fixed oxygen and nitrogen flow rate of 92 and 350 ml min^{-1}, respectively. Fig. 2 shows the power density dependence of a fuel cell with an active surface of 10 mm^2 annealed in the furnace at a constant temperature of 740 °C, which corresponds to a fuel cell temperature of 779 °C and a constant fuel cell voltage of 0.4 V. A current density appears at a critical CH_4 flow rate value of ~55 ml min^{-1} and increases with CH_4 partial pressure until a $P(CH_4)/P(O_2)$ ~1 ratio is attained. Then, power density fuel cell remains constant and higher CH_4 partial pressures do not increase the power density of the fuel cell. The fuel cell power density increases until a maximum constant value which corresponds to ~300 mW cm^{-2} when the CH_4/O_2 ratio is >1. Similar results have been observed by other authors using YSZ as electrolyte [21]. The origin of this behaviour was attributed to oxidation and reduction cycles ongoing on the nickel surface that depends on the oxygen concentration of the gas mixture. We have observed that catalytic measurements carried out on isolated powders of the same catalyst in the same reactor at similar experimental conditions show that the H_2 production by the catalyst decreases when the CH_4/O_2 ratio is also <1. Probably, the H_2 generated by the catalyst reacts with the additional O_2 from the atmosphere in these conditions giving H_2O as reaction product of the methane oxidation. Normally, the H_2 generated in the anode reacts with electrochemical oxygen produced in the cathode at CH_4/O_2 ratio >1 in a single-chamber fuel cell at our experimental conditions. Nevertheless, some H_2 produced in the anode reacts directly with the O_2 from the atmosphere when the CH_4/O_2 ratio is <1 and the powder density decreases drastically. We have observed that this critical CH_4/O_2 ratio depends on temperature, internal diameter of the reactor tube and on the total flux rate of the carrier gas for our CGO electrolytes. Oxidation and reduction cycles ongoing on the CGO electrolytes (Ce^{+4} to Ce^{+3}) could also be happen at our experimental temperatures. For this reason, further research is carried out in our laboratory in order to understand this behaviour.

In another series of experiments, we have explored the influence of the total flux rate of the carrier gas for a constant CH_4:O_2:N_2 gases composition. Furnace temperature and voltage load were maintained also constant at 740 °C and 0.4 V, respectively. Fig. 3 shows the power density dependence of the fuel cell as a function of total flow rate for a fixed CH_4:O_2:N_2 ratio of 0.9:1:3.8 at a constant furnace temperature and voltage load. We have observed that the power density increases progressively with the total flow rate indicating that the reaction is controlled by diffusion process. Probably the elimination of reaction products like H_2O and CO_2 through the porosity of the anode by the stirring rate increases the power density of the fuel cells. We have observed that the O.C.V. is not very sensitive to the flux rate variation. On the other hand, the fuel cell temperature increases only a few degrees (from 768 to 779 °C) for 266 and 525 ml min^{-1}, respectively. The increase in the fuel cell temperature by the total flux rate of the carrier gas at a constant furnace temperature is due to the exothermic character of the reaction, but cannot to explain the drastic power density increase of the fuel cells.

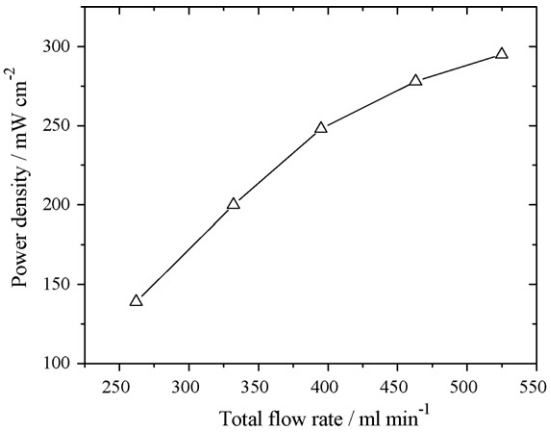

Fig. 3. Power density at 0.4 V and 740 °C furnace temperature (cell temperature changes from 768 to 779 °C for 266 and 525 ml min^{-1}, respectively) as a function of total flow rate for a fixed CH_4:O_2:N_2 ratios of 0.9:1:3.8.

The peaks power densities for a fuel cell operating at 694, 732 and 779 °C, which correspond to a furnace temperatures of 650, 700 and 740 °C at a constant total flux rate of 525 ml min^{-1} are represented in Fig. 4. We have explored higher temperatures at the same atmosphere, but the density power drops drastically to zero, because the H_2 produced in the anode reacts directly with the O_2 from the atmosphere as occurs when we decrease the CH_4/O_2 ratio to <1 at lower temperatures (see above). Similar limit in the temperature has been found by other authors in ~20 μm thin films

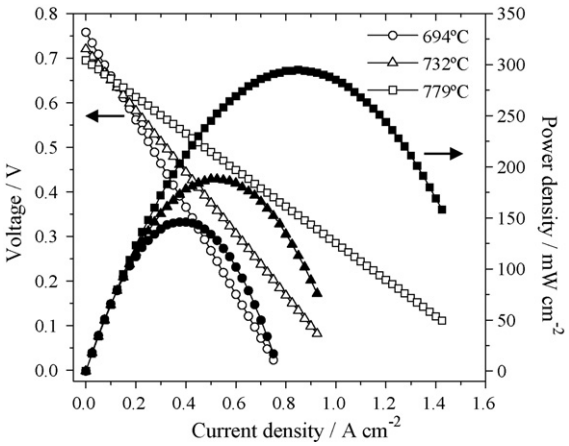

Fig. 4. Cell voltage and power density as function of current density for a fuel cell of CGO electrolyte-supported (thickness = 200 μm), Ni–CGO as anode and LSCO–CGO–AgO as cathode.

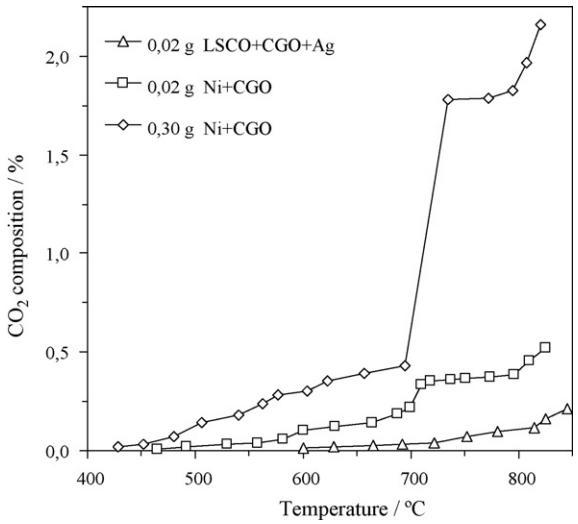

Fig. 5. Catalytic activity of LSCO + CGO + AgO (0.02 g, calcined at 900 °C) and Ni + CGO (0.02 g and 0.30 g, reduced at 1000 °C) for methane oxidation to CO_2 (CO_2 produced from methane flow rate of 100 ml min^{-1} and CH_4:O_2:N_2 ratios of 1.1:1:3.8).

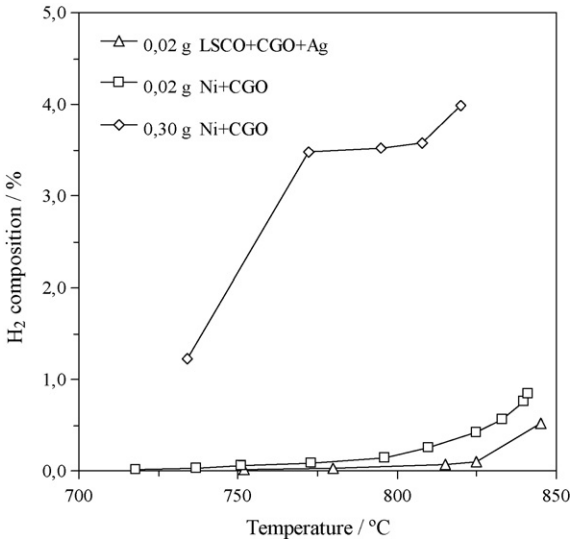

Fig. 6. Catalytic activity of LSCO + CGO + AgO (0.02 g, calcined at 900 °C) and Ni + CGO (0.02 g and 0.30 g, reduced at 1000 °C) for methane oxidation to H_2 (H_2 concentracion produced from methane flow rate of 100 ml min^{-1} and CH_4:O_2:N_2 ratios of 1.1:1:3.8).

SDC (787 °C in contrast to 779 °C) at a similar methane to oxygen ratio of ~1:1 [11]. A maximum power density peak of 760 mW cm^{-2} was found by these authors to be compared with the 280 mW cm^{-2} measured in our fuel cell for an electrolyte of 200 μm thickness. Nevertheless, the experimental conditions as the carrier gas (He respect to N_2), flux rates and geometry of the reactor were not the same. For this reasons, it is not possible to compare the power density of the fuel cells. In Fig. 4, we can see that the current density drops linearly with voltage load and the peak of the power density is symmetrical and increases with temperature. On the hand, the O.C.V. is lower for the methane fed single-chamber fuel cells than for propane single-chamber fuel cells (0.75 V respect to 0.85 V for propane fed SOFCs) because the working temperatures are higher (650–775 °C respect to 450–550 °C, respectively) [13]. Probably, substantial reduction of Ce^{+4} to Ce^{+3} at high temperature (methane fed fuel cells) contributes to this reduction in the O.C.V. Ce^{+4} ions are stable below 600 °C (propane fed fuel cells), but Ce^{+3} ions, which lead to n-type conductivity, appear at higher temperatures and decrease the O.C.V. because the GDC electrolyte becomes a mixed conductor [20]. The Ni/CGO anode and the LSCO/CGO/AgO cathode seem to be stable under these experimental conditions. Nevertheless, more long term behaviour and cycling properties must to be undertaken in order to determine the veritable stability of the fuel cells here studied in a flowing mixture of methane (100 ml min^{-1}) and synthetic air (442 ml min^{-1}).

3.3. Catalytic measurements

Catalytic research is necessary to understand the mechanisms involved in these types of fuel cell. So, we have investigated the catalytic activity of both electrodes: Ni + CGO (anode) and LSCO + CGO + AgO (cathode) in the methane oxidation reaction at the same experimental conditions than the operating fuel cells. For this reason, we have studied the catalytic activity of similar quantities of anode and cathode powders used in the fuel cells but introduced in a gold crucible. Fig. 5 shows the CO_2 production for 20 and 300 mg of powders of Ni + CGO in front of the methane oxidation into the same reactor and at the same experimental conditions. We have also represented in the same figure the CO_2 production for 20 mg of LSCO + CGO + AgO which is the estimated quantity used in the cathodes of the fuel cells. We can see that catalytic activity of the cathode (LSCO + CGO + AgO) is negligible in front of the activity of the anode (Ni + CGO) in the range of temperatures considered for the fuel cells (650–775 °C). CO_2 production by the anode composition appears at 400 °C and increases continuously with temperature until ~720 °C. Then, the CO_2 production increases drastically at higher temperatures. On the other hand, CO_2 production is detected at ~600 °C for the LSCO + CGO + AgO cathode, but a substantial increase take place only at temperatures up to 830 °C. On the other hand, H_2 production by the anode and cathode compositions is represented in Fig. 6. Hydrogen generation appears at ~700 °C and ~830 °C for the anode and cathode compositions, respectively. These temperatures correspond approximately to the drastic increase in the CO_2 concentration represented in Fig. 5. So, we have observed the appearance of the O.C.V. and considerable density currents in the fuel cells at the same temperature where H_2 is generated by the Ni catalyst ~690 °C (see Fig. 7). We can conclude that the generation of H_2 by the partial oxidation of methane on the anode produces the voltage and density currents of the single-chamber fuel cells studied here.

This effect has been also reported for LSCO powders in a previous work and has been attributed to a change in the reaction mechanism, which corresponds at the pass from the total oxidation of methane giving $CO_2 + H_2O$ to a partial oxidation of methane giving mainly $CO_2 + H_2$ [22]. This change in the reaction mechanism is due

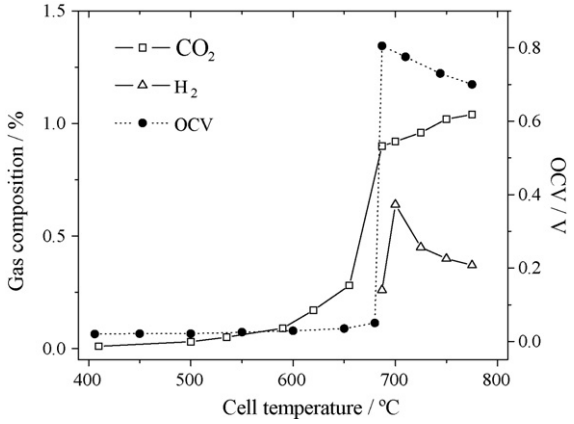

Fig. 7. Open circuit voltage (O.C.V.), CO_2 and H_2 composition as function of cell temperature for a fixed methane flow rate of 100 ml min^{-1} and air flow rate of 442 ml min^{-1}.

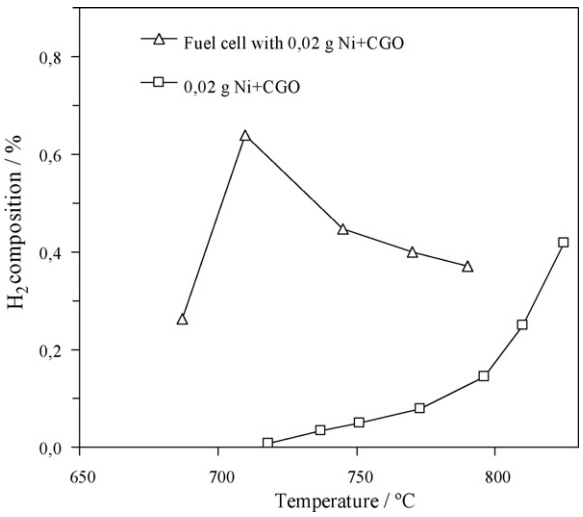

Fig. 8. Hydrogen composition produced by a fuel cell with 0.02 g of Ni + CGO as anode and by 0.02 g of isolated powders of Ni + CGO (methane flow rate = 100 ml min^{-1} and CH_4:O_2:N_2 = 1.1:1:3.8).

to the decomposition of the cobaltite giving metallic cobalt, SrO and La_2O_3 [23].

Finally, we have observed an apparent electrocatalytic effect in the fuel cells. The same quantity of catalyst produces different values in the H_2 concentration of the atmosphere, depending if the catalyst is as isolated powder form in a gold crucible or it is deposited as anode in a polarized fuel cell. Fig. 8 shows the H_2 production inside the reactor when 20 mg of Ni + CGO are used in powder form or as a painted anode on a polarized single chamber fuel cell. When the isolated powders of the catalyst are used, the H_2 appears spontaneously at higher temperature (~720 °C) than in polarized fuel cells (~685 °C). H_2 production increases continuously with the temperature when isolated powders of anode are used. However, H_2 generation appears drastically at 700 °C for a single-chamber fuel cell and its concentration decreases continuously with temperature. This critical temperature corresponds to the apparition of the maximum open circuit voltage (O.C.V.) of the fuel cells. Then, CO_2, H_2 concentration and the O.C.V. values decrease progressively with temperature, probably because some Ce^{+4} is reduced to Ce^{+3} and the electrocatalytic effect decreases. The O.C.V. drops to zero at higher fuel cell temperatures (T > 800 °C). Probably, the homogeneous reaction takes place in the reactor atmosphere as have been explained above. So, there are a lower and an upper temperature limit for the single-chamber fuel cells which correspond to the H_2 generation by the anode or to the homogeneous reaction in the atmosphere, respectively. The same behaviour was observed in propane fed single-chamber SOFCs at lower working temperatures due to the reactivity of this hydrocarbon at lower temperatures on the same catalyst [13].

4. Conclusions

The $La_{0.5}Sr_{0.5}CoO_{3-\delta}$ (LSCO) is a stable cathode in diluted methane–air atmospheres for single-chamber solid oxide fuel cells based on CGO electrolytes at temperatures as high as 780 °C. There is a considerable difference between the temperature of the furnace and the temperature of the fuel cells due to the exothermic character of the methane oxidation on the anode. It is possible to increase the temperature difference between the furnace and the single-chamber fuel cells by increasing the insulation of the reactor. So, the heating produced by the partial oxidation of methane could be used to help to maintain the fuel cell operational conditions. Electrical properties of the fuel cells depend substantially on the atmosphere composition (PCH_4/PO_2 ratio) and on the flux rates of the total carrier gases, but the optimization of the parameters is possible in order to obtain good power densities. So, single-chamber electrolyte-supported fuel cells are a promising alternative for the fabrication of intermediate temperature solid oxide fuel cells operating between 650 and 780 °C in methane-diluted atmospheres. There is an electrocatalytic effect produced by the polarization of the fuel cells, because the same quantity of Ni + CGO catalyst increases the H_2 production by the methane partial oxidation, depending if the catalyst is deposited as anode in a fuel cell or as isolated powder form in an inert crucible.

Acknowledgements

The present work was financed by the Spanish MCTE under Projects MAT2006-11080-C02-02, MAT2006-12904-C02-01 and MAT2007-66403-C02-01, as well as XaRMAE (Xarxa de Referència en Materials Avançats per a l'Energia, Generalitat de Catalunya) and the aid of the Commissioner for the University and Investigation of the University Department of Innovation and Company of the Catalan Autonomous Government of Catalonia and the European Social Fund.

References

[1] W. van Gool, Philips Res. Rep. 20 (1965) 81.
[2] G.A. Lousi, J.M. Lee, D.L. Maricle, J.C. Trocciola, U.S. Pat. 4,248,941 (1981).
[3] C.K. Dyer, Nature 343 (1990) 547.
[4] P.T. Moseley, D.E. Williams, Nature 346 (1990) 23.
[5] T. Hibino, K. Asano, H. Iwahara, Chem. Lett. 1131 (1993).
[6] I. Riess, P.J. van der Putand, J. Schoonmam, Solid State Ionics 82 (1995) 1.
[7] T. Hibino, S. Wang, S. Kakimoto, M. Sano, Electrochem. Solid State Lett. 2 (7) (1999) 317.
[8] T. Hibino, et al., Science 288 (2000) 2031–2033.
[9] Z. Shao, S.M. Haile, J. Ahn, P.D. Ronney, Z. Zhanand, S.A. Barnett, Nature 435 (2005) 795.
[10] Z. Shao, S.M. Haile, Nature 431 (2004) 170–173.
[11] Z.P. Shao, J. Mederos, W.C. Chueh, S.M. Haile, J. Power Sources 162 (2006) 589–596.
[12] Y. Hao, Z. Shao, J. Mederos, W. Lai, D.G. Goodwin, S.M. Haile, Solid State Ionics 177 (2006) 2013–2021.
[13] S. Piñol, M. Morales, F. Espiell, J. Power Sources 169 (2007) 2–8.
[14] B.C.H. Steele, Solid State Ionics 129 (2000) 95–110.
[15] L. Minervini, M.O. Zacate, R.W. Grimes, Solid State Ionics 116 (1999) 339–349.
[16] H. Yahiro, K. Eguchi, H. Arai, Solid State Ionics 36 (1989) 71–75.
[17] K. Eguchi, T. Setoguchi, T. Inoue, H. Arai, Solid State Ionics 52 (1992) 165–172.
[18] I. Riess, D. Braunshtein, D.S. Tannhauser, J. Am. Ceram. Soc. 64 (1981) 480.
[19] S. Piñol, Fuel Cells Sci. Technol. 4 (2006) 434–437.
[20] D. Pérez-Coll, D. Marrero-López, P. Núñez, S. Piñol, J.R. Frade, Electrochim. Acta 51 (2006) 6463–6469.
[21] X. Jacques-Bénard, T.W. Napporn, R. Roberge, M. Meunier, J. Power Sources 153 (2006) 108–113.
[22] S. Piñol, M. Morales, F. Espiell, J. New Mater. Electrochem. Syst. 11 (2008) 119–124.
[23] R. Lago, G. Bini, M.A. Peña, L.G. Fierro, J. Catal. 167 (1997) 198–209.